



Research paper

A renal-cerebral-peripheral sympathetic reflex mediates insulin resistance in chronic kidney disease



Wei Cao^{a,1}, Meng Shi^{a,1}, Liling Wu^a, Zhichen Yang^a, Xiaobing Yang^a, Hongfa Liu^a, Xin Xu^a, Youhua Liu^a, Christopher S. Wilcox^{b,**}, Fan Fan Hou^{a,*}

^a Division of Nephrology, Nanfang Hospital, 1838 North Guangzhou Avenue, Guangzhou 510515, PR China.

^b Division of Nephrology and Hypertension, Georgetown University Medical Central, 3800 Reservoir Road, NW, 6 PHC Bldg, F6003, Washington, DC 20007, USA

ARTICLE INFO

Article history:

Received 10 July 2018

Received in revised form 18 October 2018

Accepted 22 October 2018

Available online 11 November 2018

Keywords:

Insulin resistance

Salt

Sympathetic reflex

Adipose tissue

Renin-angiotensin system

Chronic kidney disease

ABSTRACT

Background: Insulin resistance (IR) complicates chronic kidney disease (CKD). We tested the hypothesis that CKD activates a broad reflex response from the kidneys and the white adipose tissue to impair peripheral glucose uptake and investigated the role of salt intake in this process.

Methods: 5/6-nephrectomized rats were administered normal- or high-salt for 3 weeks. Conclusions were tested in 100 non-diabetic patients with stage 3–5 CKD.

Findings: High-salt in 5/6-nephrectomized rats decreased insulin-stimulated 2-deoxyglucose uptake >25% via a sympathetic nervous system (SNS) reflex that linked the IR to reactive oxygen species (ROS) and the renin-angiotensin system (RAS) in brain and peripheral tissues. Salt-loading in CKD enhanced inflammation in adipose tissue and skeletal muscle, and enhanced the impairment of insulin signaling and Glut4 trafficking. Denervation of the kidneys or adipose tissue or deafferentation of adipose tissue improved IR >40%. In patients with non-diabetic CKD, IR was positively correlated with salt intake after controlling for cofounders ($r = 0.334$, $P = 0.001$) and was linked to activation of the RAS/SNS and to impaired glucose uptake in adipose tissue and skeletal muscle, all of which depended on salt intake.

Interpretation: CKD engages a renal/adipose-cerebral-peripheral sympathetic reflex that activates the RAS/ROS axes to promote IR via local inflammation and impaired Glut4 trafficking that are enhanced by high-salt intake. The findings point to a role for blockade of RAS or α - and β -adrenergic receptors to reduce IR in patients with CKD.

Fund: National Natural Science Foundation of China.

© 2018 The Authors. Published by Elsevier B.V. This is an open access article under the CC BY-NC-ND license (<http://creativecommons.org/licenses/by-nc-nd/4.0/>).

1. Introduction

Insulin resistance (IR) accompanies not only type 2 diabetes but also non-diabetic chronic kidney disease (CKD) [1], where it increases the risk of premature mortality [2], cardiovascular events [3], and progression of renal disease [4]. However, the mechanisms underlying IR in CKD remain unclear. Skeletal muscle has long been considered the major site of insulin-stimulated glucose uptake *in vivo*. However, insulin also lowers blood glucose by suppressing hepatic glucose production and by increasing adipose glucose uptake [5]. Indeed, CKD is associated with impaired insulin-stimulated glucose uptake and post-receptor

insulin signaling in adipose tissue [6] in addition to skeletal muscle [7]. Since IR is a potentially modifiable cardiovascular disease risk factor in patients with even early CKD [8], it is important to unravel the underlying mechanisms.

IR accompanies salt-sensitivity in rodents [9] and humans [10]. Patients with CKD are prone to salt-sensitive hypertension [11]. High-salt intake also is reported to increase IR in the general population [12,13] and obese subjects [14], but it remains unclear if IR in CKD is enhanced by dietary salt.

We reported recently that a high-salt diet fed in a 5/6-nephrectomized (5/6Nx) rat model of CKD caused renal inflammation and fibrosis that depended on a renal-cerebral renin-angiotensin system (RAS) axis driven by reactive oxygen species (ROS) via a robust intercommunication provided by the afferent and efferent renal sympathetic nervous system (SNS) [15]. Therefore, we used this 5/6Nx rat model to investigate the hypothesis that CKD activates a renal-cerebral-peripheral reflex to generate ROS and Ang II in skeletal muscle and adipose tissue that impairs their glucose uptake and thereby

* Division of Nephrology, Nanfang Hospital, 1838 North Guangzhou Avenue, Guangzhou 510515, PR China.

** Division of Nephrology and Hypertension, Georgetown University Medical Central, 3800 Reservoir Road, NW, 6 PHC Bldg, F6003, Washington, DC 20007, USA

E-mail addresses: wilcoxch@georgetown.edu (C.S. Wilcox), ffhouguangzhou@163.com (F.F. Hou).

¹ These authors contributed equally to this work.

Research in context

Evidence before this study

Insulin resistance (IR) complicates chronic kidney disease (CKD) by unknown mechanisms.

Added value of this study

This study of CKD (5/6-nephrectomized rats) demonstrates that IR is initiated by afferent nervous signals from kidneys and adipose tissue that engage a cerebral-peripheral sympathetic reflex that activates the renin-angiotensin system (RAS)/reactive oxygen species (ROS) axes to promote IR *via* local inflammation and impaired insulin signaling. This is enhanced during high-salt intake in rats with CKD, whereas similarly, a high-salt intake is shown to exacerbate IR in patients with non-diabetic CKD.

Implications of all the available evidence

IR contributes to the excess burden of cardiovascular disease in CKD. We found that IR in CKD dependent on an activation of the sympathetic nervous system (SNS) reflex and is enhanced by a high-salt intake. This points to a modifiable factor to exacerbate IR in patient with CKD.

promotes IR, and, furthermore, that this process is exacerbated by a high-salt intake.

2. Materials and methods

Details of the biochemical and molecular biology methods are available in the Supplementary Materials.

2.1. Animal experiments

All animal experiments were approved by the Institutional Animal Ethics Committee (No. NFYY-2014-05). Five-week-old male Sprague-Dawley rats (Nanfang Hospital Animal Experiment Center, China) were housed in plastic cages (3–5 per cage) at 24 ± 1 °C, 12/12 h controlled light conditions with *ad-libitum* access to water and food, unless indicated. The number of rats required was estimated by a power calculation using data from our prior studies with this model [15].

2.1.1. Protocol 1

Five-sixths nephrectomy (5/6Nx) or sham operation (sham) was performed at 6 weeks of age as previously described [16]. After operation, all rats received normal-salt diet for eight weeks, and were randomly assigned thereafter to two groups ($n = 6$ per group) receiving normal-salt (0.4% NaCl) or high-salt (4% NaCl) diet [17–19] (Trophic Animal Feed High-tech Co., Ltd., China) for 3 weeks.

2.1.2. Protocol 2

Rats with 5/6Nx were fed a high-salt (4% NaCl) diet for 3 weeks, and were randomly assigned to 12 groups ($n = 6$ in each group) for the following treatments: [1] Intragastric (IG) vehicle (phosphate buffered saline, pH 7.4) as a IG control, or IG losartan (Sigma, MO, USA) at 1 or 500 mg/kg/d to block the angiotensin (Ang) II type 1 (AT1) receptors [15]; [2] Intracerebroventricular (ICV) vehicle (artificial cerebrospinal fluid, aCSF) as a ICV control or ICV losartan at 1 mg/kg/d to block central RAS using Alzet osmotic minipumps (Durect Corp, CA, USA) [15]; [3] ICV tempol at 4.5 µg/kg/d to block central ROS using osmotic minipumps [15]; [4] ICV clonidine (Sigma) to block central sympathetic outflow at

5.76 µg/kg/d using osmotic minipumps [15]; [5] Renal denervation to block both efferent and afferent SNS signals [15]; [6] Denervation of epididymal fat pads to block both efferent and afferent SNS signals [20]; [7] Selective deafferentation of epididymal fat pads by injection of resiniferatoxin (RTX, Sigma) into bilateral epididymal fat pads as previously described with minor modification [21]; [8] IG hydralazine (Sigma) at 15 mg/kg/d to normalize blood pressure as a control for the effects of hypertension [15].

The doses of IG or ICV drugs were chosen from our previous study [15]. The accuracy of the ICV injection was confirmed by brain distribution of Evans blue. Denervation of epididymal fat pads was performed as described previously [20]. Effectiveness of denervation in epididymal adipose was demonstrated by reduction of norepinephrine (NE) levels to <30% of the control in adipose tissue. RTX-mediated selective deafferentation of epididymal fat pads was performed according to a previous report with minor modification [21]. Briefly, the bilateral epididymal fat pads were exposed and injected with RTX (20 pmol/µl, 8 µl/site, 4 sites for each fat pad). Effectiveness of deafferentation was confirmed by reduction of calcitonin gene related peptide (CGRP), an afferent nerve-specific marker, to <30% of the control in adipose tissue (Supplementary Fig. S6, a–d).

2.2. Evaluation of insulin resistance

Homeostasis model assessment of IR (HOMA-IR) was calculated using the following formulae: $\text{HOMA-IR} = \text{fasting serum insulin } (\mu\text{U/L}) \times \text{fasting serum glucose } (\text{mmol/L}) / 22.5$ [22]. A hyperinsulinemic-euglycemic clamp study was performed in conscious and unstressed rats as described previously [23]. Hepatic glucose production was calculated by subtraction of the glucose infusion rate from whole body glucose disposal [23]. At 120 min after the clamp, rats received an intravenous bolus of 2 [¹⁴C] deoxyglucose (2 [¹⁴C]DG; Perkin Elmer, MA, USA). Thirty minutes after the bolus, samples of white adipose tissue (epididymal adipose tissue) and skeletal muscle (gastrocnemius) were excised to determine the tissue-specific glucose uptake [23].

2.3. Measurement of tissue perfusion

At the end of hyperinsulinemic-euglycemic clamp studies, the blood perfusion of epididymal adipose tissue and hindlimb adductor muscle group (adductor magnus and semimembranosus) were determined by contrast-enhanced ultrasound, as previously described [24]. Initially, an epididymal fat pad was exposed and kept moist with saline. A hindlimb adductor muscle group was visualized *in situ* and identified by B-mode imaging as previously reported [25]. Contrast imaging in the epididymal fat pad and the hindlimb adductor muscle group was recorded during continuous infusion of microbubbles *via* the tail vein at 8×10^7 /min. Infusion time *versus* video intensity (VI), which is the “brightness” of pixels in the ultrasound image in decibels, was fitted to an exponential function: $y = A(1 - e^{-\beta t})$. Where, t is the infusion time, A is the plateau, VI is an index of blood volume, and β is a measure of mean microbubble velocity. Perfusion was calculated by multiplying A and β .

2.4. Antibodies

Primary antibodies used in animal studies were listed as follows: Na⁺/K⁺-ATPase α 1 subunit (05–369, Millipore, CA, USA), glucose transporter 4 (Glut4, 2213, Cell Signaling Technology, MA, USA), insulin receptor substrate 1 (IRS1, sc-559, TX, Santa Cruz Biotechnology), phosphotyrosine (sc-7020, Santa Cruz Biotechnology, USA), phosphorylated AS160 (Tyr642) (4288, Cell Signaling Technology), total AS160 (07–741 Millipore), tumor necrosis factor (TNF α , ab6671, Abcam, MA, USA), ED-1 (MCA341, Serotec, Oxford, UK), angiotensinogen (AGT, 28101, IBL, Gunma, Japan), AGT (A6279, ABClonal, Wuhan, China), Ang II (T-4007, Peninsula Laboratories, CA, USA), dystrophin (ab129996, Abcam), adiponectin (ab22554, Abcam), CGRP (GTX16211, Gene Tex, CA, USA),

tyrosine hydroxylase (TH, MAB318, Millipore), c-fos (ab209794, Abcam), Nox2 (ab129068, Abcam), p22^{phox} (sc-271,968, Santa Cruz Biotechnology), α_1 -adrenergic receptor (AR) (ab3462, Abcam), α_2 -adrenergic AR (CA1003, Cell Application, CA, USA), β_1 -AR (ab3442, Abcam), β_2 -AR (ab182136, Abcam), β_3 -AR (sc-1473, Santa Cruz Biotechnology). Secondary antibodies were purchased from Cell Signaling Technology.

2.5. Human studies

Human studies were approved by the Nanfang Hospital Ethics Committee (No. NFEC-2015-085). The participants gave written informed consent prior to inclusion. All subjects were identified by number, not by name. A cohort of 100 patients with non-diabetic stage 3–5 CKD was included from Nanfang Hospital. Eligible patients were those aged between 18 and 70 years old, with normal fasting blood glucose and oral glucose tolerance tests, and with estimated glomerular filtration rate (eGFR) lower than 60 ml/min/1.73m². but not receiving dialysis or kidney transplantation. We excluded those treated with medications known to affect insulin sensitivity (*i.e.* corticosteroids, immunosuppressive agents, angiotensin II receptor blockers, β -blockers). Characteristics of the patients were shown in Supplementary Table S3.

2.5.1. Salt intake and IR in patients with CKD

Partial Correlation Analysis Insulin resistance was measured by HOMA-IR and related to salt consumption determined by 24-hour urinary chloride excretion. The association between salt intake and HOMA-IR was analyzed by a partial correlation analysis adjusted by age, body mass index, triglyceride, eGFR, systolic blood pressure, and caloric intake (determined by 3-day diet records).

Salt intake and tissue RAS/ROS/SNS activation in patients with CKD To evaluate the alterations in adipose tissue and muscle from CKD patients under high-salt condition, 12 CKD patients with high-salt (>10 g/day, n = 6) or normal-salt consumption (<5 g/day, n = 6) and 12 age- and

salt-intake-matched non-CKD patients were studied (Supplementary Table S4). Omental adipose tissue and rectus abdominis from CKD patients were obtained during insertion of peritoneal dialysis catheters. Omental adipose tissue and rectus abdominis from non-CKD patients were collected during hernia surgery. Macrophage infiltration in adipose tissue sections was determined by immunohistochemistry staining using a monoclonal antibody recognizing human CD68 (1:50; MCA5709, Serotec, Oxford, UK). Expression of AGT, Nox2, and TH in homogenates of adipose tissue and skeletal muscle were detected by western blot using antibodies against human AGT (1:1000, AF3156, R&D, MN, USA), Nox2 (1:5000, ab129068, abcam), or TH (1:400, MAB318, Millipore) respectively. The levels of TH mRNA in tissue homogenates were determined by quantitative real-time PCR using TaKaRa SYBR® Premix Ex Taq™ kit (TaKaRa Biotechnology, Dalian, China) with gene specific primers (Supplementary Table S5) according to the manufacturer's instruction. Quantification was performed using the 2^{- $\Delta\Delta$ CT} method [26] and TH expression was normalized to expression of the housekeeping gene GAPDH. Insulin-stimulated 2-[³H] deoxyglucose (Perkin Elmer) uptake into the isolated muscle strips and adipose tissue explants were determined [27,28].

2.6. Statistical analysis

Continuous variables were expressed as mean \pm SD if normally distributed or median (25th percentile - 75th percentile, interquartile range) if abnormally distributed. Categorical variables were expressed as a number (%). Differences among groups were tested by one-way ANOVA or unpaired *t*-test with Bonferroni correction for multiple testing. Two-way ANOVA was used to test the differences in effects of salt-loading between sham-operated and 5/6Nx rats. The association between salt intake and HOMA-IR in patients with CKD was analyzed by a partial correlation analysis adjusted by age, body mass index, triglyceride, estimated GFR, systolic blood pressure and caloric intake.

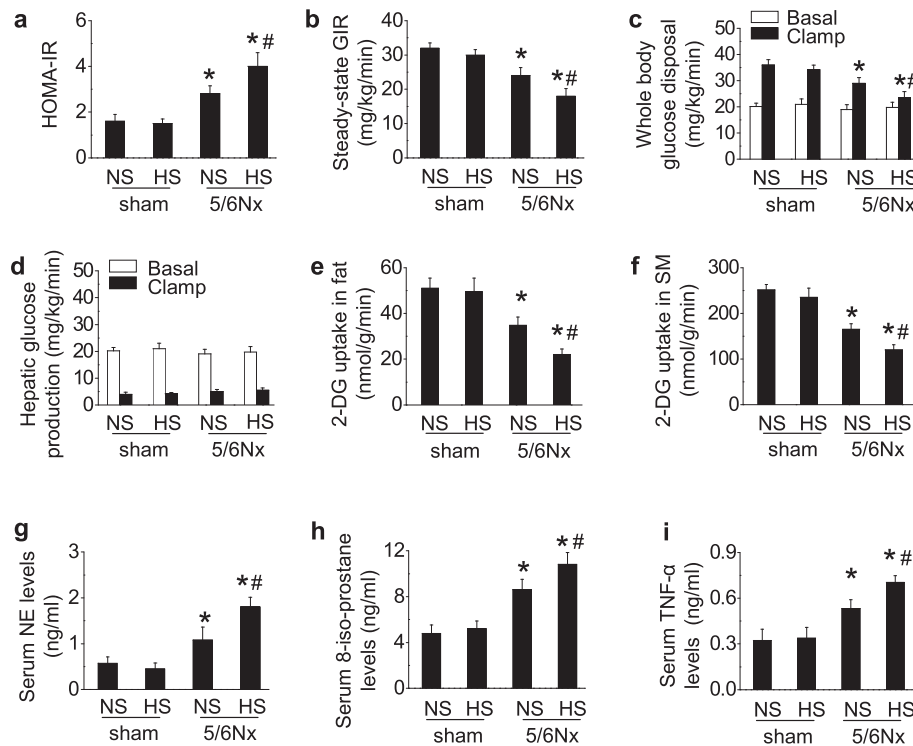


Fig. 1. CKD in rats impairs glucose uptake in adipose tissue and skeletal muscle and results in IR that are enhanced by high dietary salt. (a) Homeostasis model assessment of IR (HOMA-IR). (b) Steady-state glucose infusion rate (GIR) during hyperinsulinemic-euglycemic clamp. (c) Basal and insulin-stimulated whole-body glucose disposal. (d) Basal and insulin-stimulated hepatic glucose production. (e and f) Insulin-stimulated 2-deoxy-glucose (DG) uptake in adipose tissue (e) and skeletal muscle (SM) (f). (g–i) Serum levels of norepinephrine (NE) (g), 8-iso-prostane (h) and TNF α (i). Data are expressed as mean \pm SD (n = 6 in each group). Effects of salt-loading in all panels except d are significantly higher in 5/6Nx rats than sham-operated rats (two-way ANOVA $P < 0.05$). * $P < 0.05$ vs sham rats with the same salt intake, # $P < 0.05$ vs 5/6Nx rats on normal-salt diet by unpaired *t*-test. NS, normal salt; HS, high salt.

Statistical analysis was conducted with SPSS 17.0 for Windows. A value of $P < 0.05$ was considered statistically significant. The statistical parameters can be found in the figure legends.

3. Results

3.1. CKD in rats impairs glucose uptake in adipose tissue and skeletal muscle and results in IR that are enhanced by high dietary salt

Eight weeks after 5/6Nx or sham operations, rats were randomly divided into two groups receiving a normal-salt (0.4%NaCl) or a high-salt (4%NaCl) diet for 3 weeks. Insulin sensitivity was measured by the HOMA-IR and a hyperinsulinemic-euglycemic clamp test. IR was unchanged in sham rats but was impaired in 5/6Nx rats (Fig. 1a–c).

Compared to the sham rats, basal and insulin-stimulated hepatic glucose production were unaltered in 5/6Nx rats fed a normal- or a high-salt intake (Fig. 1d). However, insulin-stimulated glucose uptake in adipose tissue and skeletal muscle were markedly decreased in 5/6Nx rats and were decreased further by high-salt intake (Fig. 1e and f). 5/6Nx rats also had increased circulating markers of SNS activity (NE), oxidative stress (8-iso-prostane), and inflammation (TNF α) (Fig. 1g–i), and raised the systolic blood pressure (Supplementary Table S1), all of which were enhanced by high-salt intake. However, serum leptin levels were increased significantly in 5/6Nx rats, but not changed further by salt-loading (Supplementary Table S1).

The sodium content of adipose tissue or skeletal muscle was unchanged by high-salt intake in 5/6Nx rats but was increased in skin (Supplementary Table S1).

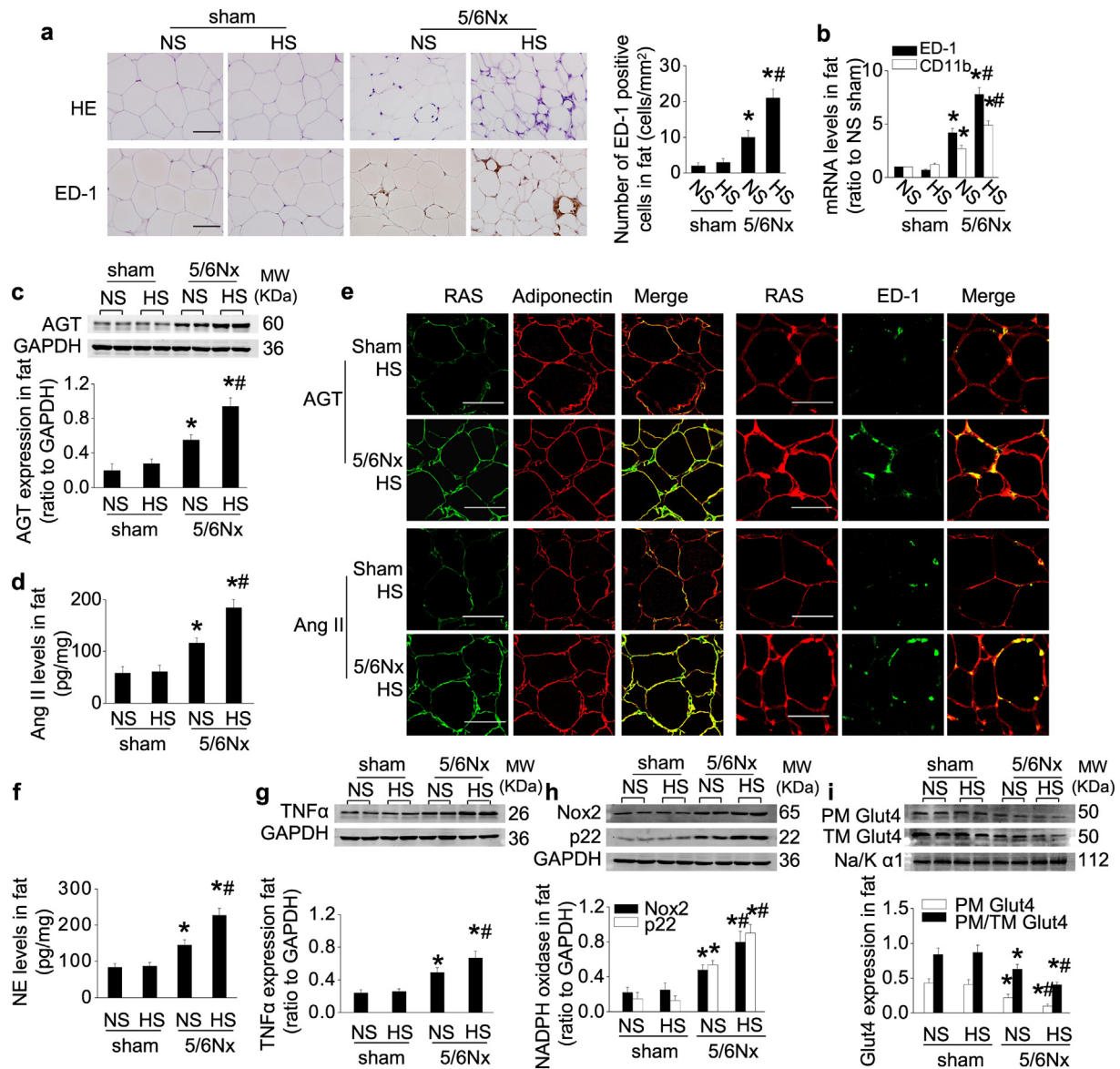


Fig. 2. CKD in rats activates the RAS and SNS in adipose tissue, resulting in inflammation and impaired Glut4 trafficking that are enhanced by high dietary salt. (a and b) Adipose macrophage infiltration: representative photos of HE staining and immunohistochemical staining of ED-1, quantitative analysis of ED-1-positive cells (a), and mRNA levels of ED-1 and CD11b (b) in adipose tissue. (c and d) Protein levels of AGT (c) and Ang II (d) in adipose tissue. (e) Localization of adipose AGT or Ang II determined by double-staining with an antibody against AGT or Ang II and an antibody recognizing adiponectin (marker of adipocyte) or ED-1 (marker of macrophage). (f–h) Norepinephrine (NE) level (f), and expression of TNF α (g) and NADPH oxidase subunit Nox2 and p22phox (h) in adipose tissue. (i) Glut4 expression in extracted plasma membrane (PM) and the ratio of PM to total membrane (TM) Glut4 under insulin stimulation. Scale bar = 100 μ m. Data are expressed as mean \pm SD ($n = 6$ in each group). Effects of salt-loading in all panels are significantly higher in 5/6Nx rats than sham-operated rats (two-way ANOVA $P < 0.05$). * $P < 0.05$ vs sham rats with the same salt intake, # $P < 0.05$ vs 5/6Nx rats on normal-salt diet by unpaired t-test.

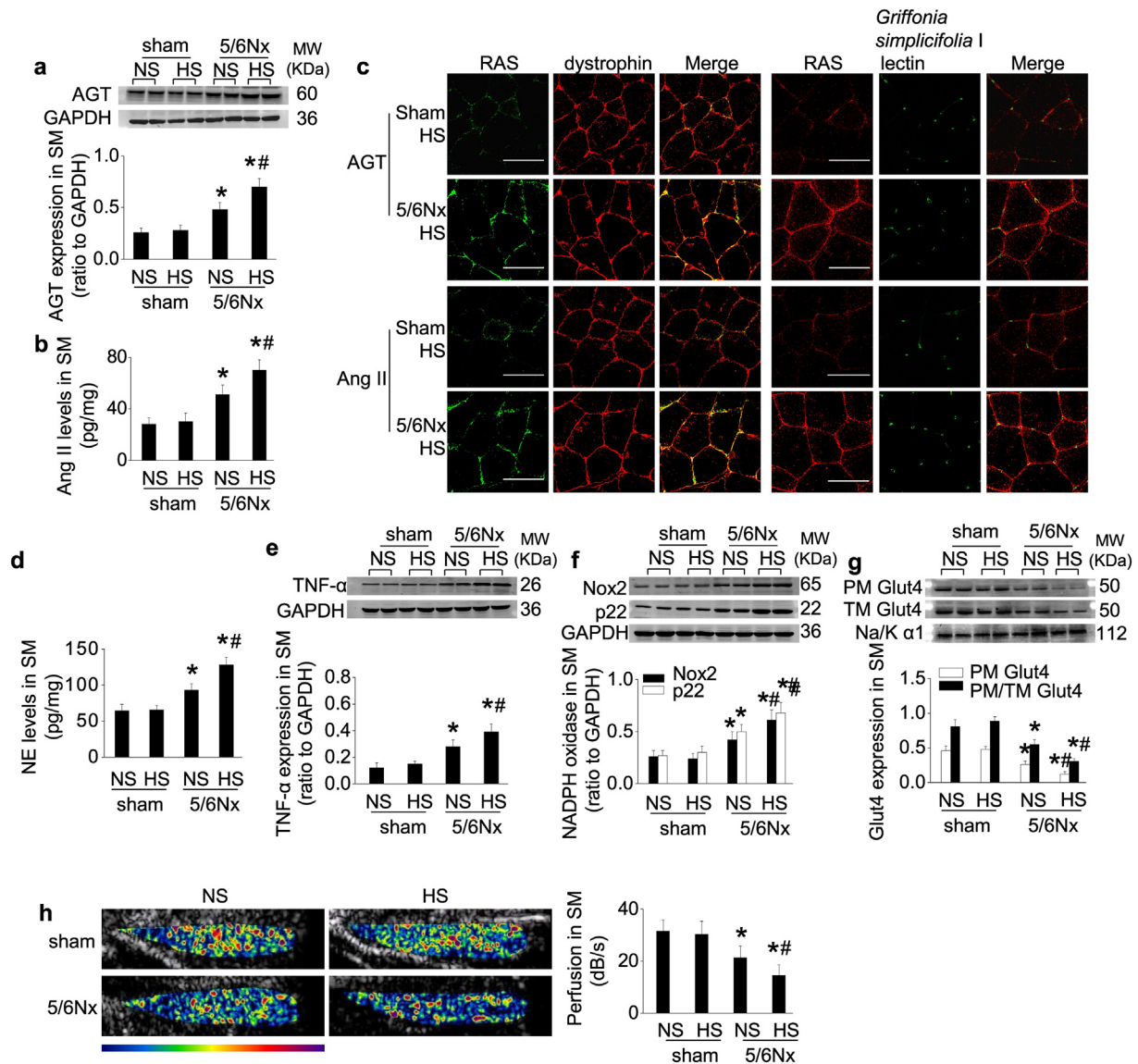


Fig. 3. CKD in rats activates RAS and SNS in skeletal muscle, reduces muscle perfusion, and impairs Glut4 trafficking that are enhanced by high dietary salt. (a and b) Protein levels of AGT (a) and Ang II (b) in skeletal muscle (SM). (c) Localization of muscle AGT or Ang II determined by double-staining with an antibody against AGT or Ang II and an antibody recognizing dystrophy (marker of myocyte) or Griffonia simplicifolia I lectin (marker of microvessel). (d–f) Norepinephrine (NE) level (d), and expression of TNF α (e) and NADPH oxidase subunit Nox2 and p22phox (f) in SM. (g) Glut4 expression in extracted plasma membrane (PM) and the ratio of PM to total membrane (TM) Glut4 under insulin stimulation. (h) Hindlimb perfusion measured by contrast-enhanced ultrasound under insulin stimulation. Scale bar = 100 μ m. Data are expressed as mean \pm SD (n = 6 in each group). Effects of salt-loading in all panels are significantly higher in 5/6Nx rats than sham-operated rats (two-way ANOVA P < 0.05). *P < 0.05 vs sham rats with the same salt intake, #P < 0.05 vs 5/6Nx rats on normal-salt diet by unpaired t-test.

3.2. CKD in rats activates the RAS and SNS in adipose tissue, resulting in inflammation and impaired Glut4 trafficking that are enhanced by high dietary salt

5/6Nx rats had significantly increased macrophage infiltration in white adipose tissue that was enhanced by dietary salt (Fig. 2a and b).

Expression of AGT and Ang II in adipose tissue were located mainly in adipocytes and infiltrating macrophages (Fig. 2e). They were unchanged by salt loading in sham rats but were upregulated in 5/6Nx rats and were increased further by high-salt intake (Fig. 2c–e; Supplementary Fig. S1a–c). Circulating levels of Ang II were reduced by CKD and by high-salt intake (Supplementary Table S1). But CKD increased the adipose tissue concentrations of NE and TNF α , and upregulated nicotinamide adenine dinucleotide phosphate (NADPH) oxidase subunits

Nox2 and p22^{phox}, all of which were enhanced by high dietary salt (Fig. 2f–h; Supplementary Fig. S1d).

The adipose expression and translocation of Glut4 were downregulated in 5/6Nx rats, and were reduced further by high-salt intake (Fig. 2i; Supplementary Fig. S1e). Adipose Glut4 transcription is activated by the CCAAT/enhancer binding protein- α (C/EBP- α) [29], whose expression paralleled that of Glut4 (Supplementary Fig. S1f). Insulin-stimulated tyrosine phosphorylation of the IRS1 and AS160 were decreased in 5/6Nx rats, particularly in those with high-salt intake (Supplementary Fig. S1g and h). However, neither 5/6Nx nor salt-loading changed insulin binding and insulin-stimulated autophosphorylation of the insulin receptor β subunit (IR β) (Supplementary Fig. S1i and j). Neither CKD nor high dietary salt altered adipose tissue blood perfusion (Supplementary Fig. S1k).

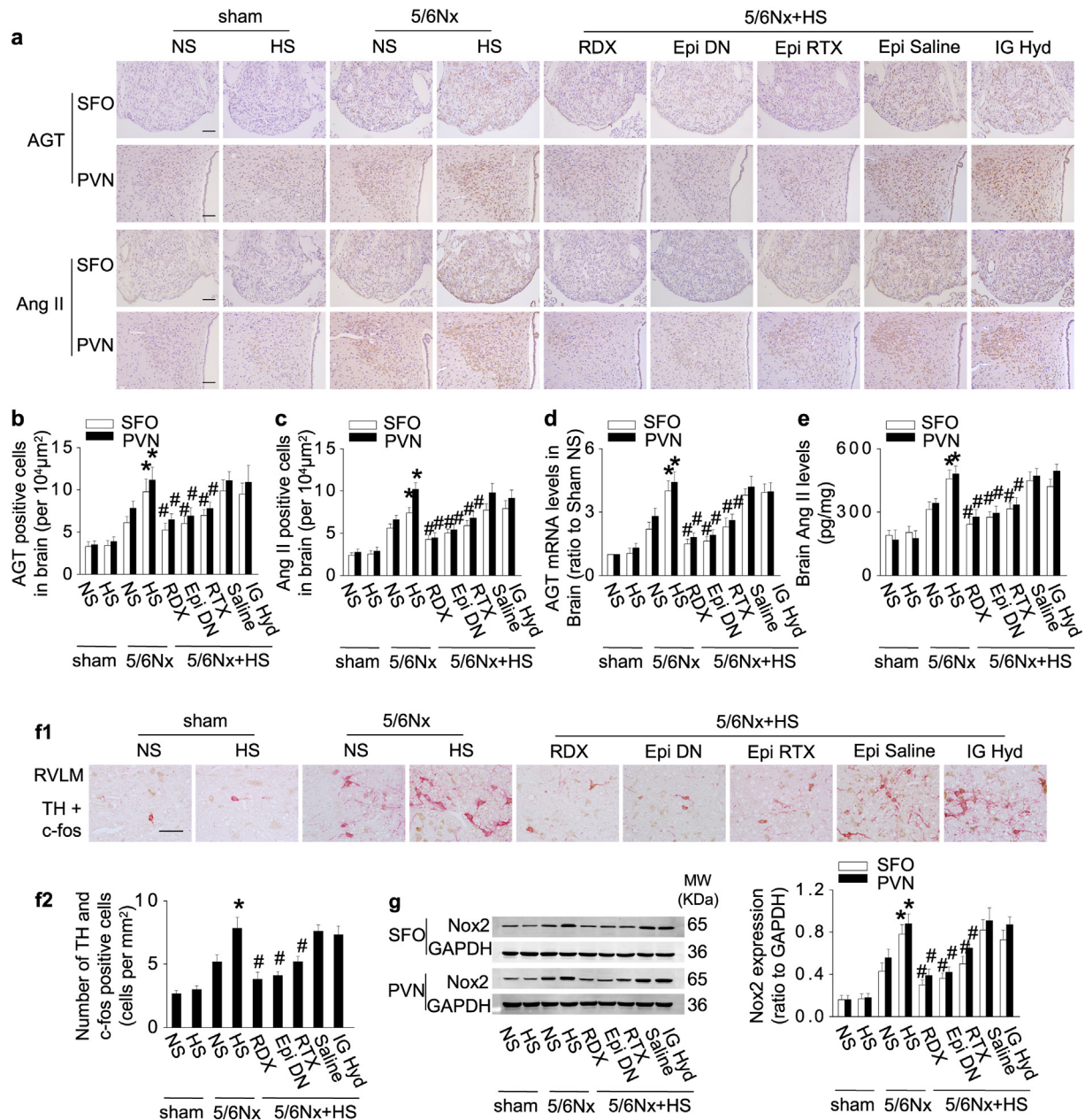


Fig. 4. CKD in rats activates the cerebral RAS and TH expression *via* signals from the innervated kidney and adipose tissue that are enhanced by high dietary salt. (a–e) Central RAS expression in sham and 5/6Nx rats with normal- or high-salt intake. Renal denervation (RDX), denervation of epididymal adipose tissue (Epi DN), or deafferentation of epididymal adipose tissue with resiniferatoxin (Epi RTX) downregulates expression of central RAS in the subfornical organ (SFO) and paraventricular nucleus (PVN): representative photos of immunohistochemistry staining (a), quantitation of AGT or Ang II-positive cells (b&c), mRNA levels of AGT (d), and the protein levels of Ang II in brain (e). (f) Expression of tyrosine hydroxylase (TH) in c-fos positive neurons in rostral ventrolateral medulla (RVLM). (g) Expression of Nox2 in brain. Scale bar = 100 μ m. Data are expressed as mean \pm SD ($n = 6$ in each group). Effects of salt-loading in all panels are significantly higher in 5/6Nx rats than sham-operated rats (two-way ANOVA $P < 0.05$). * $P < 0.05$ vs 5/6Nx rats on normal-salt diet, # $P < 0.05$ vs 5/6Nx rats on high-salt diet by unpaired t-test. Epi Saline, injection of vehicle (saline) into bilateral epididymal fat pads.

3.3. CKD in rats activates RAS and SNS in skeletal muscle, reduces muscle perfusion, and impairs Glut4 trafficking that are enhanced by high dietary salt

Unlike adipose tissue, cellular inflammation was not observed in skeletal muscle of 5/6Nx rats (Supplementary Fig. S2a and b) but the expression of AGT and Ang II was upregulated in both myocytes and microvessels surrounding muscle fibers (Fig. 3a–c; Supplementary Fig. S2c–e), accompanied by increased expression of NE, TNF α and NADPH oxidase subunits in skeletal muscle (Fig. 3d–f; Supplementary Fig. S2f).

The expression and translocation of Glut4 and the expression of myocyte enhancer factor 2A (MEF2A), that is a transcriptional regulator for muscle Glut4 gene [29], were reduced in skeletal muscle from 5/6Nx

rats and were reduced further by high-salt intake (Fig. 3g; Supplementary Fig. S2g and h). As in adipocytes, CKD impaired the post-receptor insulin signaling (Supplementary Fig. S2i–l) and reduced insulin-stimulated hindlimb blood perfusion in 5/6Nx rats that were exacerbated by high-salt intake (Fig. 3h).

3.4. CKD in rats activates the cerebral RAS and TH expression *via* signals from the innervated kidney and adipose tissue that are enhanced by high dietary salt

The expression and activity of the brain RAS were increased in 5/6Nx rats and enhanced by a high-salt intake in the paraventricular nucleus (PVN) and subfornical organ (SFO) (Fig. 4a–e). The expression of RAS

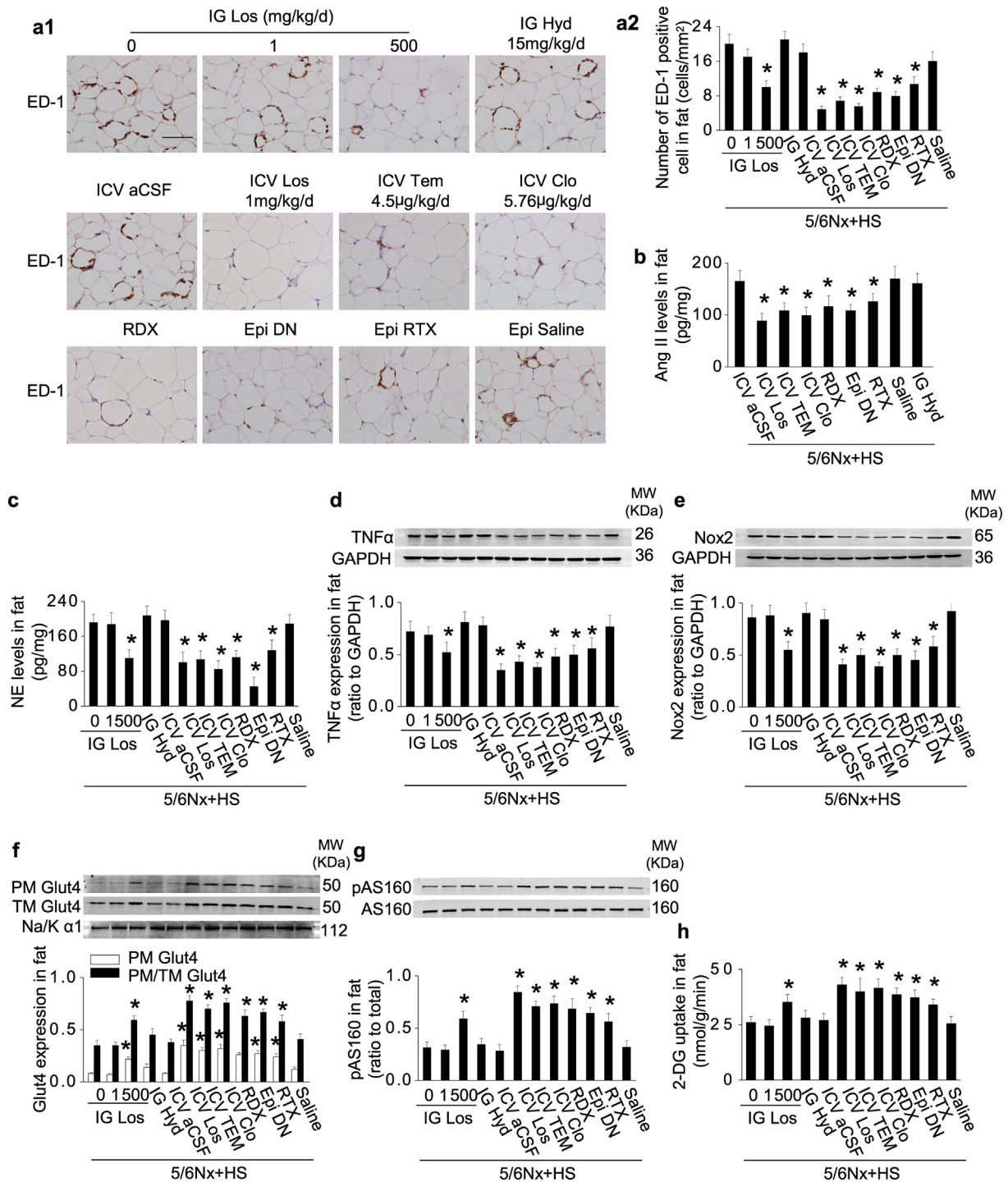


Fig. 5. Activation of adipose RAS and impaired Glut4 trafficking in 5/6Nx rats with high-salt intake are prevented by blockade of a renal-cerebral-adipose sympathetic reflex. (a) Increased adipose macrophage infiltration in 5/6Nx rats under high-salt condition was inhibited by intracerebroventricular administration (ICV) of losartan or clonidine, denervation of the kidneys (RDX) or epididymal fat pads (Epi DN), or deafferentation of epididymal fat pads with resiniferatoxin (Epi RTX). (b) Protein levels of Ang II in adipose tissue. (c–e) Norepinephrine (NE) level (c), and expression of TNFα (d) and Nox2 (e) in adipose tissue. (f) Glut4 expression in extracted plasma membrane (PM) and the ratio of PM to total membrane (TM) Glut4 under insulin stimulation. (g) Insulin-stimulated phosphorylation of AS160 in adipose tissue. (h) Insulin-stimulated 2-deoxy-glucose (DG) uptake in adipose tissue. Scale bar = 100 μm. Data are expressed as mean ± SD (n = 6 in each group). *P < 0.05 vs 5/6Nx rats under high-salt condition given vehicle (0 mg/kg/d inhibitor) by unpaired t-test.

in the brain cortex (as a control) was modest and independent of salt intake (data not shown). 5/6Nx also increased central sympathetic drive indicated by increased generation of TH in c-fos-positive neurons in the rostral ventrolateral medulla (RVLM), and induced central oxidative stress indexed by upregulation of Nox2, all of which were enhanced by high dietary salt (Fig. 4f and g).

Remarkably, denervation of the epididymal fat pads or selective blockade of epididymal fat afferent signals by RTX was as effective

as renal denervation in alleviating the upregulation of the brain RAS, TH, and Nox2 by CKD and the enhanced effect of high-salt intake (Fig. 4).

We did not consider it ethical to study the effects of muscle denervation, because this procedure causes severe distress [30]. The activation of the central RAS, SNS and oxidative stress were independent of hypertension, because their overexpression persisted after normalizing blood pressure with hydralazine (Fig. 4).

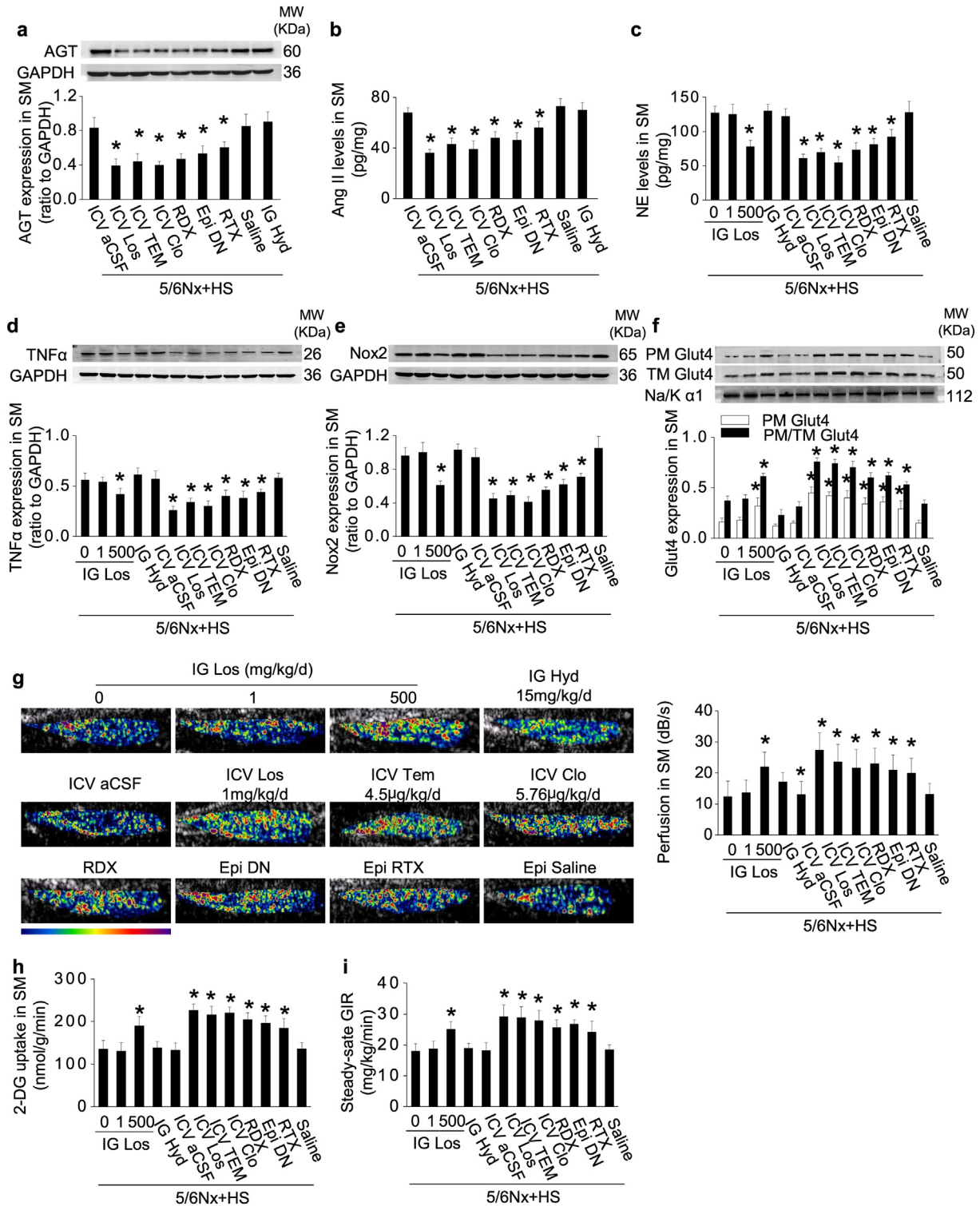


Fig. 6. Activation of the RAS/ROS and impaired Glut4 trafficking in the skeletal muscle of 5/6Nx rats with high-salt intake are prevented by blockade of a renal/adipose-cerebral-muscle sympathetic reflex. (a and b) Overexpression of skeletal muscle (SM) AGT (a) and Ang II (b) in 5/6Nx rats under high-salt condition was inhibited by intracerebroventricular administration (ICV) of losartan or clonidine, denervation of the kidneys (RDX) or epididymal fat pads (Epi DN), or deafferentation of epididymal fat pads with resineratoxin (Epi RTX). (c–e) Norepinephrine (NE) level(c), and expression of TNFα (d) and Nox2 (e) in SM. (f) Glut4 expression in extracted plasma membrane (PM) and the ratio of PM to total membrane (TM) Glut4 under insulin stimulation. (g) Hindlimb perfusion measured by contrast-enhanced ultrasound under insulin stimulation. (h) Insulin-stimulated 2-deoxyglucose (DG) uptake in SM. (i) Steady-state glucose infusion rate (GIR) during hyperinsulinemic-euglycemic clamp. Data are expressed as mean ± SD (n = 6 in each group). *P < 0.05 vs 5/6Nx rats under high-salt condition given vehicle (0 mg/kg/d inhibitor) by unpaired t-test.

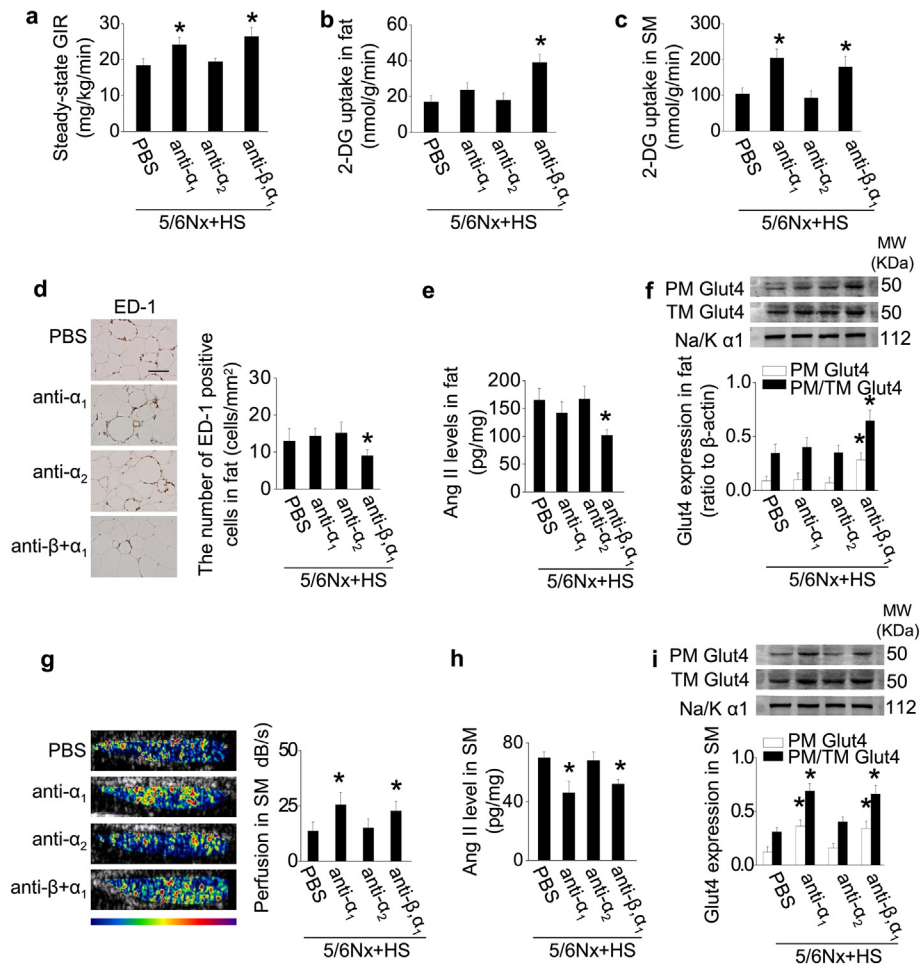


Fig. 7. Adrenergic receptors mediate IR in rats with CKD under high-salt condition. To further confirm the role of SNS in IR in 5/6Nx rats under high-salt condition, CKD rats on high-salt diet were treated with α 1-adrenergic receptor (AR) antagonist (anti- α 1; prazosin), or α 2-AR antagonist (anti- α 2; atipamezole), or β - and α 1-AR antagonist (anti- β , α 1; carvedilol) for 3 weeks. (a) Steady-state glucose infusion rate (GIR) during hyperinsulinemic-euglycemic clamp. (b and c) Insulin-stimulated 2-deoxy-glucose (DG) uptake in adipose tissue (b) and skeletal muscle (SM) (c). (d) Macrophage infiltration in adipose tissue: representative photos of immunohistochemical staining of ED-1, and quantitative analysis of ED-1-positive cells. (e) Levels of Ang II in adipose tissue. (f) Adipose Glut4 expression in extracted plasma membrane (PM) and the ratio of PM to total membrane (TM) Glut4 under insulin stimulation. (g) Hindlimb perfusion measured by contrast-enhanced ultrasound under insulin stimulation. (h) Levels of Ang II in SM. (i) SM Glut4 expression in extracted PM and the ratio of PM to TM Glut4 under insulin stimulation. Scale bar = 100 μ m. Data are expressed as mean \pm SD ($n = 6$ in each group). * $P < 0.05$ vs 5/6Nx rats under high-salt condition given vehicle (PBS) by unpaired t-test.

3.5. Activation of adipose RAS and impaired Glut4 trafficking in 5/6Nx rats with high-salt intake are prevented by blockade of a renal-cerebral-adipose sympathetic reflex

Blockade of brain AT1 receptors in 5/6Nx rats with high-salt intake by ICV administration of losartan, at a dose of 1/500 of the effective IG dose, decreased the overexpression of adipose AGT, Ang II and NE, alleviated the inflammation in adipose tissue (Fig. 5a–e; Supplementary Fig. S3a–c) and improved Glut4 trafficking, insulin signaling, and insulin-stimulated adipose glucose uptake (Fig. 5f–h; Supplementary Fig. S3d–f).

Blockade of central sympathetic outflow by ICV clonidine, or blockade of sympathetic afferent signals from the kidneys or epididymal fat pads all suppressed adipose inflammation and improved glucose uptake in 5/6Nx rats under high-salt condition (Fig. 5), whereas normalization of blood pressure with hydralazine was ineffective. Adipose inflammation and macrophage infiltration were doubled in 5/6Nx rats under high-salt condition but these were reduced by 52% by renal denervation, 56% by denervation of epididymal fat pads, by 46% with deafferentation of epididymal fat pads, and over by 60% by ICV losartan, clonidine, or tempol. Insulin-stimulated glucose uptake in adipose tissue was decreased by 60% in 5/6Nx rats during a high-salt intake but

this was restored by ICV losartan, clonidine, or tempol, or by renal denervation or by deafferentation of epididymal fat pads. These results demonstrate that impaired insulin sensitivity in adipose tissue in this model of CKD under high-salt condition is initiated by afferent neural signals arising in the kidneys and adipose tissue that induce adipose inflammation.

3.6. Activation of the RAS/ROS and impaired Glut4 trafficking in the skeletal muscle of 5/6Nx rats with high-salt intake are prevented by blockade of a renal/adipose -cerebral-muscle sympathetic reflex

The ICV administration of losartan to 5/6Nx rats under high-salt condition decreased the expression of AGT, Ang II, NE, TNF α and Nox2 (Fig. 6a–e; Supplementary Fig. S4a) and increased the expression and translocation of Glut4 (Fig. 6f; Supplementary Fig. S4b and c) and enhanced the blood perfusion (Fig. 6g) accompanied by improved insulin signaling and insulin-stimulated glucose uptake in skeletal muscle (Fig. 6h; Supplementary Fig. S4d and e).

Blockade of sympathetic traffic in 5/6Nx rats under high-salt condition by ICV clonidine, denervation of the kidneys or epididymal fat pads, or blockade of central oxidative stress by ICV tempol all reduced the overexpression of the skeletal muscle RAS, TNF α , or Nox2, preserved

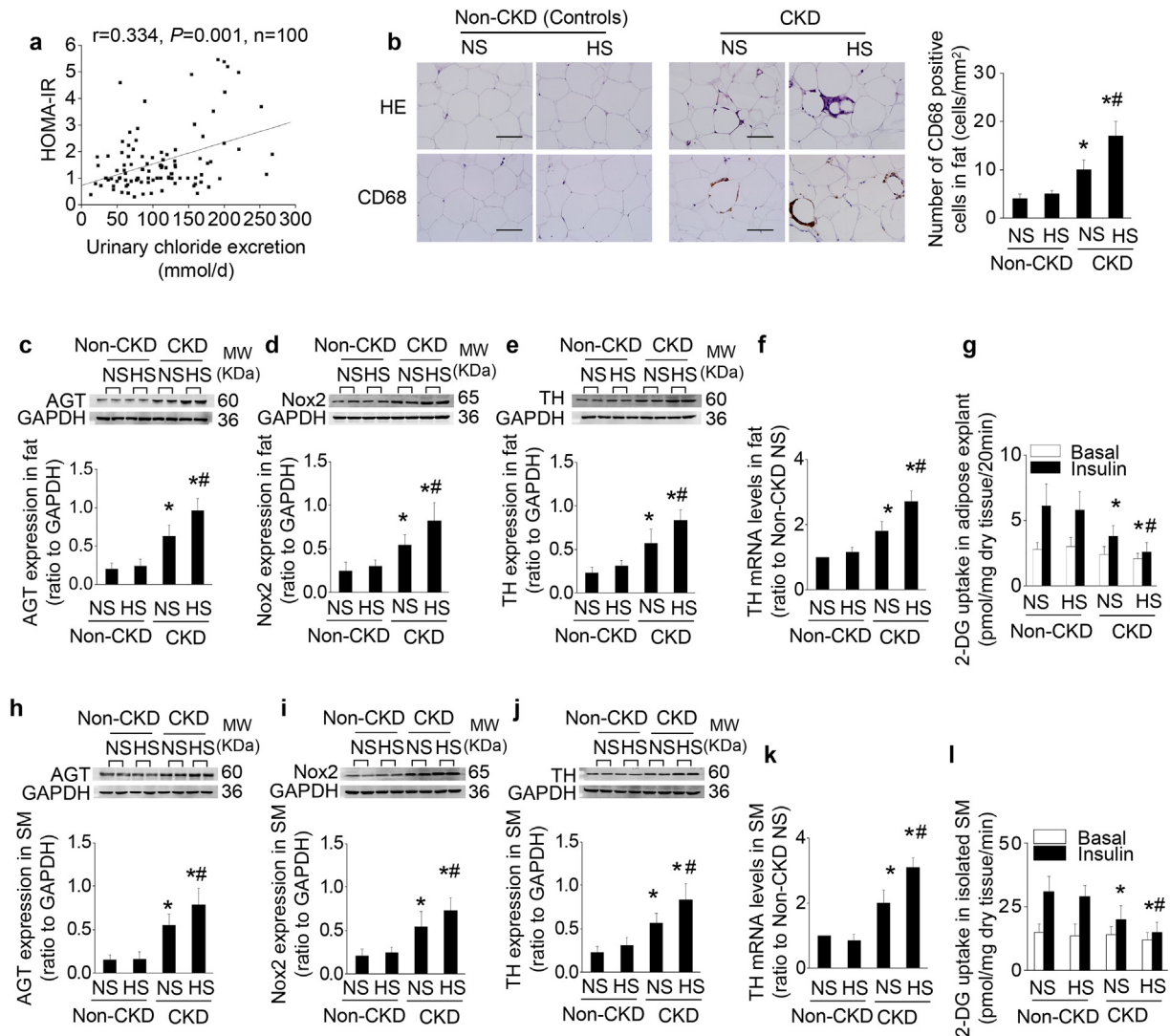


Fig. 8. The level of salt intake determines IR in non-diabetic patients with stage 3–5 CKD. (a) Correlation between daily urinary chloride excretion and the score of HOMA-IR after adjusting for age, body mass index, triglyceride, eGFR, systolic blood pressure, and caloric intake in 100 non-diabetic patients with CKD stage 3–5 using a partial correlation analysis. (b–l) To evaluate the alterations in adipose tissue and skeletal muscle (SM) in CKD under high-salt condition, tissue samples from predialysis patients with normal-salt (<5 g/day) or high-salt (>10 g/day) intake are compared with age- and salt intake-matched non-CKD patients (controls). Compared to CKD patients with normal salt consumption, CKD patients with high-salt consumption exhibit increased adipose inflammation (b), overexpression of AGT, Nox2, and TH in adipose tissue (c–f) and skeletal muscle (h–k), and impaired insulin-stimulated glucose uptake in adipose tissue explants (g) and isolated muscle strips (l). Scale bar = 100 μ m. Data are expressed as mean \pm SD in b–l ($n = 6$ in each group). Effects of salt-loading in all panels are significantly higher in CKD patients than non-CKD patients (two-way ANOVA $P < 0.05$). * $P < 0.05$ vs non-CKD patients (controls), # $P < 0.05$ vs CKD patients with normal salt diet in b–l by unpaired t -test.

muscle blood perfusion, and improved Glut4 trafficking and glucose uptake (Fig. 6). Overall, insulin-stimulated skeletal muscle glucose uptake was decreased by 40% in 5/6Nx rats under high-salt condition but this was increased >60% by ICV losartan, clonidine or tempol and >40% by renal or epididymal fat pad denervation, suggesting a robust, but not exclusive, role for the renal/adipose-cerebral-muscle sympathetic reflex to impair the skeletal muscle response to insulin in this model. Muscle insulin sensitivity was dependent on afferent neural inputs from adipose tissue since blockade of adipose afferents alone reduced NE levels and improved glucose uptake in skeletal muscle (Fig. 6).

3.7. Blockade of renal-cerebral-adipose/muscle sympathetic reflex in 5/6Nx rats with high-salt intake improves whole-body IR

Insulin sensitivity, measured by the euglycemic-clamp test, was decreased by 25% in 5/6Nx rats under high-salt condition but this was improved by >55% by ICV losartan, clonidine, or tempol, >45% by renal denervation, and >33% by denervation or deafferentation of epididymal

fat pads (Fig. 6i) that also decreased circulating levels of NE, 8-iso-prostane, and TNF α (Supplementary Table S2).

3.8. Adrenergic receptors mediate IR in rats with CKD under high-salt condition

As described previously [31], β_1 - and β_3 -ARs were the major ARs expressed in rat white adipose tissue, whereas α_1 - and β_2 -ARs were the major ARs in skeletal muscle. Their expression was unaltered by 5/6Nx or by salt loading (Supplementary Fig. S5a and b).

5/6Nx rats under high-salt condition were treated for 3 weeks with prazosin to block α_1 -AR, atipamezole to block α_2 -AR, or carvedilol to block β - and α_1 -AR. Prazosin and carvedilol improved IR in 5/6Nx rats under high-salt condition (Fig. 7a). Increased adipose inflammation, Ang II expression, Glut4 trafficking, and glucose uptake in 5/6Nx rats under high-salt condition were improved by carvedilol (Fig. 7b, d–f; Supplementary Fig. S5d), while these alterations in skeletal muscle

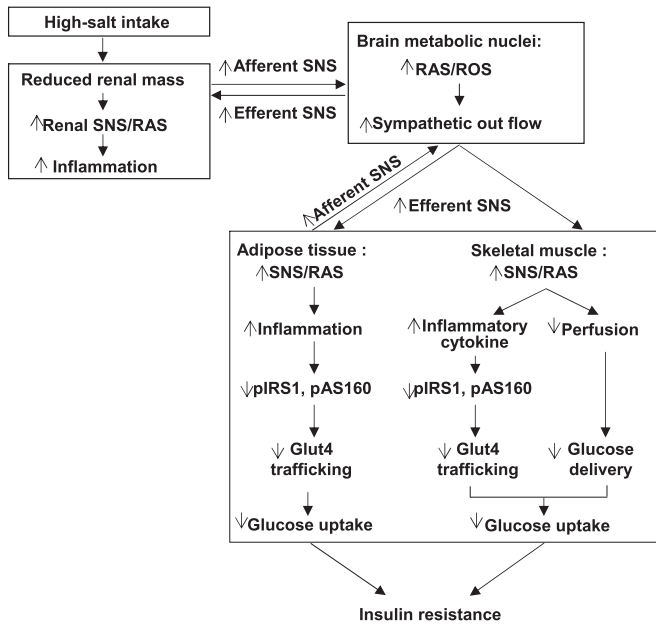


Fig. 9. The schematic diagram summarizing the steps that link a CKD in rats to insulin resistance. CKD activates the afferent sympathetic drive from the kidney and adipose tissue to the peripheral tissues that reduces the insulin-stimulated glucose uptake. This acts in a positive feedback mode to interlink the RAS/ROS systems in the brain with the RAS/ROS system in the tissues responsible for glucose disposal (adipose tissue and skeletal muscle) and thereby to mediate insulin resistance in CKD, and its enhancement by a high-salt intake.

were improved by both prazosin and carvedilol (Fig. 7c, g–i; Supplementary Fig. S5e and f).

3.9. The level of salt intake determines IR in non-diabetic patients with stage 3–5 CKD

The HOMA-IR was assessed in 100 stable non-diabetic CKD stage 3–5 patients and related to their level of salt consumption monitored from 24-hour urinary chloride excretion. The characteristics of the patients are presented in Supplementary Table S3. As shown by a partial correlation analysis (Fig. 8a), the HOMA-IR score was significantly and positively correlated with the salt intake after controlling for age, body mass index, triglyceride, eGFR, systolic blood pressure, and caloric intake. Tissue samples were compared with subjects with normal renal function matched for age and salt intake (Supplementary Table S4). The mean salt intake was 11.1 ± 0.9 g/day in normal subject during a high-salt diet. Their RAS/ROS/SNS system in adipose tissue or skeletal muscle and their insulin sensitivity were independent of salt intake. The mean salt intake in CKD patients during a high-salt diet was 11.7 ± 1.0 g/day and was 4.7 ± 0.4 g/day during a lower-salt intake. The CKD patients ingesting a high-salt intake had increased adipose inflammation, and overexpression of AGT, Nox2 and TH, and impaired glucose uptake in adipose tissue explants and isolated skeletal muscle strips (Fig. 8b–l).

4. Discussion

This study demonstrates, for the first time, that CKD activates afferent neural signals from the kidneys and from the adipose tissue, both of which increase efferent sympathetic drive to adipose tissue and skeletal muscle that reduces their insulin-stimulated glucose uptake. As illustrated in the schematic diagram (Fig. 9), this effect is driven by a high-salt intake and acts in a positive feedback mode to interlink the RAS/ROS systems in the brain with those in the adipose tissue and skeletal muscle. This reflex mechanism may also mediate IR in patients with non-diabetic CKD especially during high-salt intake.

IR is common in non-diabetic CKD [1], but the links between a damaged kidney and impaired glucose uptake have not been well studied. We found that 5/6Nx induced cellular inflammation in adipose tissue in the absence of hyperglycemia, and activated the RAS/ROS systems in both adipose tissue and skeletal muscle. High-salt intake in this CKD model further enhanced the activity of the RAS/ROS systems in these tissues. Both local inflammation and oxidative stress can impair insulin signaling and Glut4 trafficking in myocytes and adipocytes [32–34]. Although salt-loading reduced circulating Ang II levels, it paradoxically enhances the local RAS in the skeletal muscle, while adipose tissues, and cerebral nuclei that regulate autonomic and metabolic functions [35,36]. ROS can increase neuronal Ang II [15] and Ang II can increase neuronal ROS [37] in a positive feedback mode. The activation of the RAS/ROS systems in peripheral tissues in 5/6Nx rats under high-salt condition and the associated IR were largely prevented by blockade of the central RAS or ROS. Thus the central and peripheral RAS/ROS system occupy a pivotal role in IR, consistent with previous reports that blockade of AT1 receptors improves IR in patients with CKD [38] and blockade of ROS with tempol improves IR in rats [39].

This study has disclosed a previously unrecognized rich neural network in CKD enhanced by high-salt intake that is driven by afferent impulses from the damaged kidneys and white adipose tissue and coordinates a reduction in peripheral glucose uptake. This is supported by several lines of evidence. First, the expression of TH, which is the rate-limiting enzyme for NE synthesis, was increased in the RVLM of 5/6Nx rats fed a high-salt diet. The RVLM is the gateway for activation of the SNS [40], indicating increased central sympathetic drive in this model. Second, activation of the peripheral SNS was confirmed by increased NE in the adipose tissue and skeletal muscle in both 5/6Nx rats and patients with CKD, particularly during high-salt intake. Importantly, over-activation of the central and peripheral RAS/ROS systems and impaired peripheral glucose uptake were all improved by interruption of this sympathetic reflex either by central blockade of SNS outflow, or by denervation of the kidneys or adipose tissue. Thus, the kidney/adipose-brain-muscle reflex is a critical mediator of the impaired insulin sensitivity in this model. Interestingly, adipose tissue deafferentation restored glucose uptake and blood perfusion in skeletal muscle, and suppressed the local RAS/ROS/SNS, suggesting that adipose tissue contributes to sensing and coordinating the adverse metabolic effects of salt intake in CKD. Previous studies have reported that salt-loading increases IR in spontaneously hypertensive rats [41,42]. Our study extends this to a metabolic link dependent on the SNS among damaged a kidney, brain, and the tissues responsible for glucose disposal.

An important question is whether CKD impairs IR by activating the SNS to reduce peripheral blood flow and hence glucose delivery or by inhibiting cellular glucose uptake. The impaired glucose uptake in skeletal muscle was corrected by α_1 -AR blockade by prazosin or carvedilol that also corrected the reduced blood flow. This is consistent with the reports of improved insulin sensitivity in patients treated with α_1 -AR blockers and suggests that muscle glucose uptake is limited by blood glucose delivery [43,44]. However, α -AR blockade with prazosin did not improve glucose uptake in adipose tissue. This required combined α - and β -AR blockade with carvedilol that did not change adipose tissue blood flow. Thus, different mechanisms govern the regulation of glucose uptake by the SNS in skeletal muscle and adipose tissue.

In summary, this study demonstrates that CKD leads to IR in part by activation of a renal/adipose-cerebral-peripheral RAS/ROS axis interlinked by renal, adipose tissue and skeletal muscle sympathetic nerves. Salt-loading in CKD further exacerbates this pathway via the local ROS/RAS systems that enhance the local inflammation in adipose tissue and skeletal muscle to impair insulin signaling and glucose uptake. Since IR may contribute to the excess burden of cardiovascular diseases in patients with CKD, understanding the mechanism of IR is a critical first step in efforts to reduce the risk of associated cardiovascular damage. Since many patients are unable to restrict dietary salt

intake, other approaches to prevent IR must often be sought. Our experimental study demonstrates the utility of RAS blockade with losartan or combined α and β adrenergic blockade with carvedilol to mitigate IR in this condition, independent of blood pressure. This provides a rationale for the use of these drugs in patients with CKD. Although this requires further investigation, our clinical study in such patients suggests that similar mechanisms underlie IR in patients with CKD.

Funding sources

This study was supported by the Major International (Regional) Joint Research Project of National Natural Science Foundation of China (81620108003 to F.F.H.), the National Key Technology Support Program of China (2013BAI09B06 to F.F.H.), the State Key Program of National Natural Science Foundation of China (81430016 to F.F.H.), the Foundation for Innovation Research Groups of the National Natural Science Foundation of China (81521003 to Y. L.), the National Natural Science Foundation of China (81570619 and 81870473 to W.C.), NIH (HL-68686; HL-134511; DK-049870; DK-036079 to C.S.W.) and funds from the George E. Schreiner Chair of Nephrology and the Wolters Chair of Cardiovascular Disease (to C.S.W.), the Smith-Kogard and Gildenhorn-Spiesman Family Foundation and the Georgetown University Hypertension Research Center (to C.S.W.).

Declaration of interests

None.

Author contributions

W.C. and M.S. performed the experiments, analyzed the data, and drafted part of the manuscript. L.L.W. and Z.C.Y. performed histology and biochemical experiments. X.B.Y. and H.F.L. conducted the cohort study and collected human samples. X.X. performed statistical analysis. Y.H.L. gave suggestions to the study design and paper writing, C.S.W. designed part of the experiments and revised the manuscript. F.F.H. designed and financed the study, wrote and edited the manuscript.

Appendix A. Supplementary data

Supplementary data to this article can be found online at <https://doi.org/10.1016/j.ebiom.2018.10.054>.

References

- de Boer IH, Zelnick L, Afkarian M, et al. Impaired glucose and insulin homeostasis in moderate-severe CKD. *J Am Soc Nephrol* 2016;27(9):2861–71.
- Xu H, Huang X, Arnlov J, et al. Clinical correlates of insulin sensitivity and its association with mortality among men with CKD stages 3 and 4. *Clin J Am Soc Nephrol* 2014;9(4):690–7.
- Shinohara K, Shoji T, Emoto M, et al. Insulin resistance as an independent predictor of cardiovascular mortality in patients with end-stage renal disease. *J Am Soc Nephrol* 2002;13(7):1894–900.
- Kaartinen K, Syrjanen J, Porsti I, et al. Insulin resistance and the progression of IgA glomerulonephritis. *Nephrol Dial Transplant* 2007;22(3):778–83.
- Spoto B, Pisano A, Zoccali C. Insulin resistance in chronic kidney disease: A systematic review. *Am J Physiol Renal Physiol* 2016;311(6) [F1087–F108].
- Jacobs DB, Hayes GR, Truglia JA, Lockwood DH. Alterations of glucose transporter systems in insulin-resistant uremic rats. *Am J Physiol* 1989;257(2 Pt 1):E193–7.
- Cecchin F, Itoop O, Sinha MK, Caro JF. Insulin resistance in uremia: insulin receptor kinase activity in liver and muscle from chronic uremic rats. *Am J Physiol* 1988;254(4 Pt 1):E394–401.
- Becker B, Kronenberg F, Kielstein JT, et al. Renal insulin resistance syndrome, adiponectin and cardiovascular events in patients with kidney disease: the mild and moderate kidney disease study. *J Am Soc Nephrol* 2005;16(4):1091–8.
- Ogihara T, Asano T, Ando K, et al. High-salt diet enhances insulin signaling and induces insulin resistance in Dahl salt-sensitive rats. *Hypertension* 2002;40(1):83–9.
- Mitch WE, Remuzzi G. Diets for patients with chronic kidney disease, should we reconsider? *BMC Nephrol* 2016;17(1):80.
- Johnson RJ, Herrera-Acosta J, Schreiner GF, Rodriguez-Iturbe B. Subtle acquired renal injury as a mechanism of salt-sensitive hypertension. *N Engl J Med* 2002;346(12):913–23.
- Oh SW, Han KH, Han SY, Koo HS, Kim S, Chin HJ. Association of sodium excretion with metabolic syndrome, insulin resistance, and body fat. *Medicine (Baltimore)* 2015;94(39):e1650.
- Wen W, Wan Z, Zhou D, Zhou J, Yuan Z. The amelioration of insulin resistance in salt loading subjects by potassium supplementation is associated with a reduction in plasma IL-17A levels. *Exp Clin Endocrinol Diabetes* 2017;125(8):571–6.
- Safety MoFaD. A study for association between obesity and salt intake in Korea. Cheongju: Ministry of food and drug safety; 2014.
- Cao W, Li A, Wang L, et al. A salt-induced reno-cerebral reflex activates renin-angiotensin systems and promotes CKD progression. *J Am Soc Nephrol* 2015;26(7):1619–33.
- Li HY, Hou FF, Zhang X, et al. Advanced oxidation protein products accelerate renal fibrosis in a remnant kidney model. *J Am Soc Nephrol* 2007;18(2):528–38.
- Chao J, Zhang JJ, Lin KF, Chao L. Adenovirus-mediated kallikrein gene delivery reverses salt-induced renal injury in Dahl salt-sensitive rats. *Kidney Int* 1998;54(4):1250–60.
- Declercq VC, Goldsby JS, McMurray DN, Chapkin RS. Distinct adipose depots from mice differentially respond to a high-fat, high-salt diet. *J Nutr* 2016;146(6):1189–96.
- Licican EL, McGiff JC, Pedraza PL, Ferreri NR, Falck JR, Carroll MA. Exaggerated response to adenosine in kidneys from high salt-fed rats: Role of epoxyeicosatrienoic acids. *Am J Physiol Renal Physiol* 2005;289(2):F386–92.
- Shi H, Song CK, Giordano A, Cinti S, Bartness TJ. Sensory or sympathetic white adipose tissue denervation differentially affects depot growth and cellularity. *Am J Physiol Regul Integr Comp Physiol* 2005;288(4):R1028–37.
- Xiong XQ, Chen WW, Han Y, et al. Enhanced adipose afferent reflex contributes to sympathetic activation in diet-induced obesity hypertension. *Hypertension* 2012;60(5):1280–6.
- Matthews DR, Hosker JP, Rudenski AS, Naylor BA, Treacher DF, Turner RC. Homeostasis model assessment: insulin resistance and beta-cell function from fasting plasma glucose and insulin concentrations in man. *Diabetologia* 1985;28(7):412–9.
- Kim JK. Hyperinsulinemic-euglycemic clamp to assess insulin sensitivity in vivo. *Methods Mol Biol* 2009;560:221–38.
- Wang J, Zhao Z, Shen S, et al. Selective depletion of tumor neovasculature by microbubble destruction with appropriate ultrasound pressure. *Int J Cancer* 2015;137(10):2478–91.
- Belcik JT, Davidson BP, Foster T, et al. Contrast-enhanced ultrasound assessment of impaired adipose tissue and muscle perfusion in insulin-resistant mice. *Circ Cardiovasc Imaging* 2015;8(4).
- Livak KJ, Schmittgen TD. Analysis of relative gene expression data using real-time quantitative PCR and the $2^{-\Delta\Delta C_T}$ method. *Methods* 2001;25(4):402–8.
- Dohm GL, Tapscott EB, Pories WJ, et al. An in vitro human muscle preparation suitable for metabolic studies. Decreased insulin stimulation of glucose transport in muscle from morbidly obese and diabetic subjects. *J Clin Invest* 1988;82(2):486–94.
- Stolic M, Russell A, Hutley L, et al. Glucose uptake and insulin action in human adipose tissue—influence of BMI, anatomical depot and body fat distribution. *Int J Obes Relat Metab Disord* 2002;26(1):17–23.
- Im SS, Kwon SK, Kim TH, Kim HI, Ahn YH. Regulation of glucose transporter type 4 isoform gene expression in muscle and adipocytes. *IUBMB Life* 2007;59(3):134–45.
- Bouyer LJ, Whelan PJ, Pearson KG, Rossignol S. Adaptive locomotor plasticity in chronic spinal cats after ankle extensors neurectomy. *J Neurosci* 2001;21(10):3531–41.
- Lynch GS, Ryall JG. Role of beta-adrenoceptor signaling in skeletal muscle: implications for muscle wasting and disease. *Physiol Rev* 2008;88(2):729–67.
- Wilcox CS. Effects of tempol and redox-cycling nitroxides in models of oxidative stress. *Pharmacol Ther* 2010;126(2):119–45.
- Wu Y, Wu T, Wu J, et al. Chronic inflammation exacerbates glucose metabolism disorders in C57BL/6j mice fed with high-fat diet. *J Endocrinol* 2013;219(3):195–204.
- Ramalingam L, Menikdiwela K, Lemieux M, et al. The renin angiotensin system, oxidative stress and mitochondrial function in obesity and insulin resistance. *Biochim Biophys Acta* 2017;1863(5):1106–14.
- Cruz JC, Flor AF, Franca-Silva MS, Balarini CM, Braga VA. Reactive oxygen species in the paraventricular nucleus of the hypothalamus alter sympathetic activity during metabolic syndrome. *Front Physiol* 2015;6:384.
- Cancelliere NM, Ferguson AV. Subfornical organ neurons integrate cardiovascular and metabolic signals. *Am J Physiol Regul Integr Comp Physiol* 2017;312(2) [R253–R62].
- Lob HE, Schultz D, Marvar PJ, Davison RL, Harrison DG. Role of the NADPH oxidases in the subfornical organ in angiotensin II-induced hypertension. *Hypertension* 2013;61(2):382–7.
- de Vinuesa SG, Goicoechea M, Kanter J, et al. Insulin resistance, inflammatory biomarkers, and adipokines in patients with chronic kidney disease: effects of angiotensin II blockade. *J Am Soc Nephrol* 2006;17(12 Suppl 3):S206–12.
- Bourgoin F, Bachelard H, Badaeu M, Lariviere R, Nadeau A, Pitre M. Effects of tempol on endothelial and vascular dysfunctions and insulin resistance induced by a high-fat high-sucrose diet in the rat. *Can J Physiol Pharmacol* 2013;91(7):547–61.
- Kumagai H, Oshima N, Matsuura T, et al. Importance of rostral ventrolateral medulla neurons in determining efferent sympathetic nerve activity and blood pressure. *Hypertens Res* 2012;35(2):132–41.
- Koga Y, Hirooka Y, Araki S, Nozoe M, Kishi T, Sunagawa K. High salt intake enhances blood pressure increase during development of hypertension via oxidative stress in rostral ventrolateral medulla of spontaneously hypertensive rats. *Hypertens Res* 2008;31(11):2075–83.

- [42] Takeda Y, Yoneda T, Demura M, Furukawa K, Miyamori I, Mabuchi H. Effects of high sodium intake on cardiovascular aldosterone synthesis in stroke-prone spontaneously hypertensive rats. *J Hypertens* 2001;19(3):635–9 Pt 2.
- [43] Shibasaki S, Eguchi K, Matsui Y, et al. Adrenergic blockade improved insulin resistance in patients with morning hypertension: The Japan morning surge-1 study. *J Hypertens* 2009;27(6):1252–7.
- [44] Gomes ME, Mulder A, Bellersen L, Verheugt FW, Smits P, Tack CJ. Alpha-receptor blockade improves muscle perfusion and glucose uptake in heart failure. *Eur J Heart Fail* 2010;12(10):1061–6.